Progress In Electromagnetics Research, PIER 23, 137–164, 1999

ANALYSIS OF ELECTROMAGNETIC WAVE PROPAGATION IN FOREST ENVIRONMENT ALONG MULTIPLE PATHS

L. W. Li, T. S. Yeo, P. S. Kooi, M. S. Leong, and J. H. Koh

Centre for Microwave and RF
Department of Electrical Engineering
National University of Singapore
10 Kent Ridge Crescent, Singapore 119260

1. INTRODUCTION

The presence of forest foliage causes attenuation of radio waves along a radio path and reduces the communication range of the radio equipment. In planning a communication link, quantitative knowledge of the excess transmission loss suffered by the radio waves due to the presence of the foliage is essential. Radio wave propagation in vegetated environment has been the subject of intensive studies. Those earlier studies usually considered radio propagation in forests modeled as a homogeneous and isotropic dielectric layer placed over a conducting earth [1–5]. In that analysis, the Hertz potential theory was used, and satisfactory results were obtained.

Recently, a four-layered model has been widely adopted and commonly used in the analysis of propagation mechanism in forest environments [6–8]. Two lossy dielectric layers placed over a semi-infinite ground plane are used to represent the canopy layer and trunk layer of the forest, respectively. To solve the problem of the electromagnetic wave propagation in this model, eigenfunction expansion of the dyadic Green's function is used in this paper. The use of the dyadic Green's function for the analysis of the electromagnetic wave propagation in semi-infinite media was described by Tai [9] and a generalization of these functions for the case of an N-layered medium [10], and expression for the coefficients of the scattered dyadic Green's functions in multi-layered medium have been recently obtained [11, 12]. The similar ideas developed in [13] will be also implemented inside the current paper. In [13], the analysis has been conducted only on the z-components of the electromagnetic fields due to its length restriction, so that the overall effects of the forest and the global contributions due to all the electromagnetic field components cannot be seen clearly.

In this paper, the dyadic Green's functions for the four-layered planar geometry are first determined. From these functions, *all the the electric field components* of the electromagnetic waves radiated from an inclined dipole antenna located in the trunk layer were obtained in Section 2, and then were evaluated in Section 3, using the saddle point technique which accounts for the direct and multiple reflected waves, and the branch-cut integration technique which gives contributions of lateral waves along various interfaces [14]. The transmission losses for vertical, horizontal, and 45° inclined dipoles were finally calculated numerically in Section 4 for typical forests. Also, an error occurring in the publication [5] has been pointed out and corrected in this paper.

2. FORMULATION OF THE PROBLEM

The geometry that will be considered is shown in Fig. 1. The layer II represents a medium of tree crowns (canopy) with dielectric parameters ϵ_2, μ_2 and σ_2, while layer III represents a medium of tree trunks (trunk) with dielectric parameters ϵ_3, μ_3 and σ_3. The height of layer II measured along the z-direction is H_1, while the height of layer III is H_2. Throughout the analysis, the air (layer I) and ground (layer IV) are assumed to extend to infinity, with dielectric parameters given

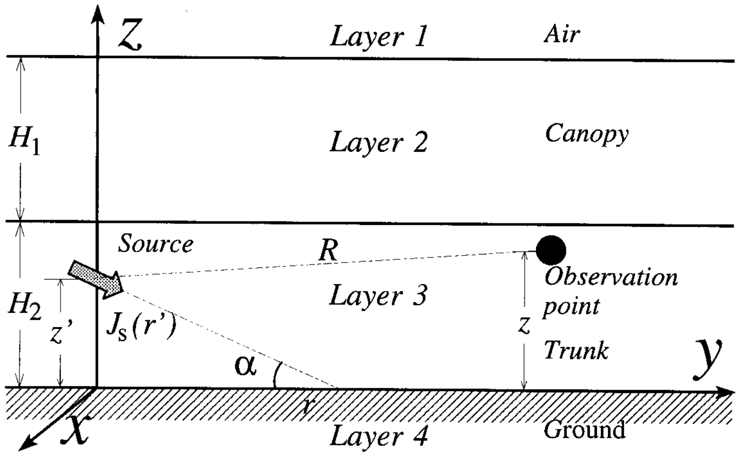

Figure 1. Geometry for the forest model of four-layers.

by ϵ_0 and μ_0, and ϵ_4, μ_4 and σ_4, respectively.

An electric dipole with an inclination angle α with respect to the boundary plane between layers and an observation point are both located in layer III. The source that feeds the electric dipole has a harmonic time dependence given by exp($-j\omega t$). The dielectric permittivities of the four layers are expressed in their complex form, [i.e., $\epsilon_\ell = \epsilon_{r\ell}\epsilon_o = \epsilon'_\ell(1 + j\sigma_\ell/\omega\epsilon'_\ell)$ where $\epsilon_{r\ell}$ ($\ell = 1, 2, 3, 4$) is the relative complex dielectric constant, σ_ℓ the conductivity of medium ℓ, and ϵ_o the free space permittivity]. The wavenumbers for the four layers are k_1 in the air semi-space, k_2 in the canopy layer, k_3 in the trunk layer, and k_4 in the semi-space ground, where $k_n = \omega\sqrt{(\mu_o\epsilon_n)}$. The magnetic permeability μ_ℓ in every layer is taken equal to that μ_0 of the free space.

The current density of an electric dipole with an inclination α with respect to the boundary plane between layers, as shown in Fig. 1, may be expressed as

$$\begin{aligned}\boldsymbol{J}_3(\boldsymbol{r}') &= (P_x\widehat{\boldsymbol{x}} + P_z\widehat{\boldsymbol{z}})[\delta(x'-0)\delta(y'-0)\delta(z'-z_o)] \\ &= [P_x(\cos\phi'\widehat{\boldsymbol{\rho}} - \sin\phi'\widehat{\boldsymbol{\phi}}) + P_z\widehat{\boldsymbol{z}}]\frac{\delta(\rho')\delta(z'-z_o)}{2\pi\rho'}, \qquad (1)\end{aligned}$$

where $z_0 = z'$ is the height of the dipole, and P_x and P_z are the horizontal and vertical dipole moments, respectively.

Using the dyadic Green's function for a four-layered planar geometry given by Li et al. [12], and following a procedure similar to that described by Cavalcante et al. [5], one obtains for the region $H_2 \geq z \geq z'$:

$$\begin{aligned}
\boldsymbol{E}_3^{>}(\boldsymbol{r}) = &-\frac{\omega\mu_3}{4\pi}\int_0^\infty \frac{d\lambda}{h_3}\Big[P_x\Big\{\big[(1+A_M^{33})\boldsymbol{M}_{o1\lambda}(h_3)+C_M^{33}\boldsymbol{M}_{o1\lambda}(-h_3)\big] \\
&\times e^{-jh_3z'}+\big[B_M^{33}\boldsymbol{M}_{o1\lambda}(h_3)+D_M^{33}\boldsymbol{M}_{o1\lambda}(-h_3)\big]e^{jh_3z'} \\
&-\frac{jh_3}{k_3}\big[(1+A_N^{33})\boldsymbol{N}_{e1\lambda}(h_3)+C_N^{33}\boldsymbol{N}_{e1\lambda}(-h_3)\big]e^{-jh_3z'} \\
&+\frac{jh_3}{k_3}\big[B_N^{33}\boldsymbol{N}_{e1\lambda}(h_3)+D_N^{33}\boldsymbol{N}_{e1\lambda}(-h_3)\big]e^{jh_3z'}\Big\} \\
&+\frac{P_z\lambda}{k_3}\Big\{\big[\left(1+A_N^{33}\right)\boldsymbol{N}_{e0\lambda}(h_3)+C_N^{33}\boldsymbol{N}_{e0\lambda}(-h_3)\big]e^{-jh_3z'} \\
&+\big[B_N^{33}\boldsymbol{N}_{e0\lambda}(h_3)+D_N^{33}\boldsymbol{N}_{e0\lambda}(-h_3)\big]e^{jh_3z'}\Big\}\Big], \qquad (2)
\end{aligned}$$

and the the region $0 \leq z \leq z'$:

$$\begin{aligned}
\boldsymbol{E}_3^{<}(\boldsymbol{r}) = &-\frac{\omega\mu_3}{4\pi}\int_0^\infty \frac{d\lambda}{h_3}\Big[P_x\Big\{\big[A_M^{33}\boldsymbol{M}_{o1\lambda}(h_3)+C_M^{33}\boldsymbol{M}_{o1\lambda}(-h_3)\big]e^{-jh_3z'} \\
&+\big[B_M^{33}\boldsymbol{M}_{o1\lambda}(h_3)+(1+D_M^{33})\boldsymbol{M}_{o1\lambda}(-h_3)\big]e^{jh_3z'} \\
&-\frac{jh_3}{k_3}\big[A_N^{33}\boldsymbol{N}_{e1\lambda}(h_3)+C_N^{33}\boldsymbol{N}_{e1\lambda}(-h_3)\big]e^{-jh_3z'} \\
&+\frac{jh_3}{k_3}\big[B_N^{33}\boldsymbol{N}_{e1\lambda}(h_3)+\left(1+D_N^{33}\right)\boldsymbol{N}_{e1\lambda}(-h_3)\big]e^{jh_3z'}\Big\} \\
&+\frac{P_z\lambda}{k_3}\Big\{\big[A_N^{33}\boldsymbol{N}_{e0\lambda}(h_3)+C_N^{33}\boldsymbol{N}_{e0\lambda}(-h_3)\big]e^{-jh_3z'} \\
&+\big[B_N^{33}\boldsymbol{N}_{e0\lambda}(h_3)+\left(1+D_N^{33}\right)\boldsymbol{N}_{e0\lambda}(-h_3)\big]e^{jh_3z'}\Big\}\Big], \qquad (3)
\end{aligned}$$

where $h_\ell = \sqrt{k_\ell^2 - \lambda^2}$ ($\ell = 1, 2, 3$ and 4), the coefficients $A_{M,N}^{33}$, $B_{M,N}^{33}$, $C_{M,N}^{33}$, $D_{M,N}^{33}$ of scattered dyadic Green's functions are expressed by Li et al. [12] and are not given here to save space.

Using the expressions for $\boldsymbol{M}_{\substack{e\\o}n\lambda}(h)$ and $\boldsymbol{N}_{\substack{e\\o}n\lambda}(h)$ (see Tai [9] and Li et al. [12]), expressions in cylindrical coordinates for the field components of (2) and (3) may be obtained as

$$\begin{bmatrix} E_{3z}^{>} \\ E_{3z}^{<} \end{bmatrix} = \frac{j\omega\mu_o}{4\pi k_3^2}\int_0^\infty \frac{\lambda^2 d\lambda}{D_3^V}\left\{P_x J_1(\lambda\rho)\cos\phi \begin{bmatrix} \Phi_{+}^{>} \\ \Phi_{-}^{<} \end{bmatrix}\right.$$
$$\left.+\frac{jP_z\lambda}{h_3}J_0(\lambda\rho)\begin{bmatrix} \Phi_{-}^{>} \\ \Phi_{+}^{<} \end{bmatrix}\right\}, \tag{4a}$$

$$\begin{bmatrix} E_{3\rho}^{>} \\ E_{3\rho}^{<} \end{bmatrix} = -\frac{\omega\mu_o}{4\pi}\int_0^\infty \frac{d\lambda}{h_3}\left\{P_x\cos\phi\left\{\frac{J_1(\lambda\rho)}{\rho}\frac{1}{D_3^H}\right.\right.$$
$$\left.\times\begin{bmatrix} \Phi_{1\rho}^{>} \\ \Phi_{1\rho}^{<} \end{bmatrix}+\left(\frac{h_3}{k_3}\right)^2\frac{dJ_1(\lambda\rho)}{d\rho}\frac{1}{D_3^V}\begin{bmatrix} \Phi_{2\rho}^{>} \\ \Phi_{2\rho}^{<} \end{bmatrix}\right\}$$
$$\left.\pm\frac{jP_z\lambda h_3}{k_3^2}\frac{dJ_0(\lambda\rho)}{d\rho}\frac{1}{D_3^V}\begin{bmatrix} \Phi_{3\rho}^{>} \\ \Phi_{3\rho}^{<} \end{bmatrix}\right\}, \tag{4b}$$

$$\begin{bmatrix} E_{3\phi}^{>} \\ E_{3\phi}^{<} \end{bmatrix} = \frac{\omega\mu_o}{4\pi}\int_0^\infty \frac{d\lambda}{h_3}P_x\sin\phi\left\{\frac{dJ_1(\lambda\rho)}{d\rho}\frac{1}{D_3^H}\begin{bmatrix} \Phi_{1\phi}^{>} \\ \Phi_{1\phi}^{<} \end{bmatrix}\right.$$
$$\left.+\left(\frac{h_3}{k_3}\right)^2\frac{J_1(\lambda\rho)}{\rho}\frac{1}{D_3^V}\begin{bmatrix} \Phi_{2\phi}^{>} \\ \Phi_{2\phi}^{<} \end{bmatrix}\right\}, \tag{4c}$$

where the intermediates $\Phi_{\pm}^{\gtrless}$ and $\Phi_{(1,2,3)(\rho,\phi)}^{\gtrless}$ are derived as

$$\Phi_{\pm}^{>} = \left[1 \pm R_3^V e^{j2h_3 z'}\right]\left\{\left[R_2^V + R_1^V e^{j2h_2H_1}\right]e^{j2h_3(H_2-z)}\right.$$
$$\left.+\left[1+R_1^V R_2^V e^{j2h_2H_1}\right]\right\}e^{jh_3(z-z')}, \tag{5a}$$

$$\Phi_{\pm}^{<} = \left[1 - R_3^V e^{j2h_3 z}\right]\left\{\left[R_2^V + R_1^V e^{j2h_2H_1}\right]e^{j2h_3(H_2-z')}\right.$$
$$\left.\pm\left[1+R_1^V R_2^V e^{j2h_2H_1}\right]\right\}e^{jh_3(z'-z)}, \tag{5b}$$

$$\Phi_{1\rho}^{>} = \left[1 - R_3^H e^{j2h_3 z'}\right]e^{jh_3(z-z')}\left\{\left[1+R_1^H R_2^H e^{j2h_2H_1}\right]\right.$$
$$\left.+\left[R_2^H + R_1^H e^{j2h_2H_1}\right]e^{j2h_3(H_2-z)}\right\}, \tag{5c}$$

$$\Phi_{1\rho}^{<} = \left[1 - R_3^H e^{j2h_3 z}\right]e^{-jh_3(z-z')}\left\{\left[1+R_1^H R_2^H e^{j2h_2H_1}\right]\right.$$
$$\left.+\left[R_2^H + R_1^H e^{j2h_2H_1}\right]e^{j2h_3(H_2-z')}\right\}, \tag{5d}$$

$$\Phi_{2\rho}^{>} = \left[1 + R_3^V e^{j2h_3 z'}\right]e^{jh_3(z-z')}\left\{\left[1+R_1^V R_2^V e^{j2h_2H_1}\right]\right.$$
$$\left.-\left[R_2^V + R_1^V e^{j2h_2H_1}\right]e^{j2h_3(H_2-z)}\right\}, \tag{5e}$$

$$\Phi_{2\rho}^{<} = \left[1 + R_3^V e^{j2h_3 z}\right] e^{-jh_3(z-z')} \left\{\left[1 + R_1^V R_2^V e^{j2h_2 H_1}\right] - \left[R_2^V + R_1^V e^{j2h_2 H_1}\right] e^{j2h_3(H_2-z')}\right\}, \tag{5f}$$

$$\Phi_{3\rho}^{>} = \left[1 - R_3^V e^{j2h_3 z'}\right] e^{jh_3(z-z')} \left\{\left[1 + R_1^V R_2^V e^{j2h_2 H_1}\right] - \left[R_2^V + R_1^V e^{j2h_2 H_1}\right] e^{j2h_3(H_2-z)}\right\}, \tag{5g}$$

$$\Phi_{3\rho}^{<} = \left[1 + R_3^V e^{j2h_3 z}\right] e^{-jh_3(z-z')} \left\{\left[1 + R_1^V R_2^V e^{j2h_2 H_1}\right] + \left[R_2^V + R_1^V e^{j2h_2 H_1}\right] e^{j2h_3(H_2-z')}\right\}, \tag{5h}$$

$$\Phi_{1\phi}^{>} = \left[1 - R_3^H e^{j2h_3 z'}\right] e^{jh_3(z-z')} \left\{\left[1 + R_1^H R_2^H e^{j2h_2 H_1}\right] + \left[R_2^H + R_1^H e^{j2h_2 H_1}\right] e^{j2h_3(H_2-z)}\right\}, \tag{5i}$$

$$\Phi_{1\phi}^{<} = \left[1 - R_3^H e^{j2h_3 z}\right] e^{-jh_3(z-z')} \left\{\left[1 + R_1^H R_2^H e^{j2h_2 H_1}\right] + \left[R_2^H + R_1^H e^{j2h_2 H_1}\right] e^{j2h_3(H_2-z')}\right\}, \tag{5j}$$

$$\Phi_{2\phi}^{>} = \left[1 + R_3^V e^{j2h_3 z'}\right] e^{jh_3(z-z')} \left\{\left[1 + R_1^V R_2^V e^{j2h_2 H_1}\right] - \left[R_2^V + R_1^V e^{j2h_2 H_1}\right] e^{j2h_3(H_2-z)}\right\}, \tag{5k}$$

$$\Phi_{2\phi}^{<} = \left[1 + R_3^V e^{j2h_3 z}\right] e^{-jh_3(z-z')} \left\{\left[1 + R_1^V R_2^V e^{j2h_2 H_1}\right] - \left[R_2^V + R_1^V e^{j2h_2 H_1}\right] e^{j2h_3(H_2-z')}\right\}; \tag{5l}$$

the reflection coefficients $R_i^{H,V}$ ($i = 1, 2$ and 3) for TE (H) mode and TM (V) mode are given respectively by

$$R_f^H = \frac{\mu_f h_{f+1} - \mu_{f+1} h_f}{\mu_f h_{f+1} + \mu_{f+1} h_f}, \tag{6a}$$

$$R_f^V = \frac{\mu_f h_f k_{f+1}^2 - \mu_{f+1} h_{f+1} k_f^2}{\mu_f h_f k_{f+1}^2 + \mu_{f+1} h_{f+1} k_f^2}; \tag{6b}$$

and the denominator $D_3^{H,V}$ is given by:

$$D_3^{V,H} = 1 + R_1^{V,H} R_2^{V,H} e^{i2h_2 H_1} + \left[R_2^{V,H} + R_1^{V,H} e^{i2h_2 H_1}\right] R_3^{V,H} e^{i2h_3 H_2}. \tag{7}$$

3. ANALYTICAL ELECTRIC FIELDS IN CLOSED FORM

To evaluate the integrals, it is convenient to convert the range of the integral from $(0 \to \infty)$ to $(-\infty \to \infty)$. Thus the Bessel functions and their derivatives need to be transformed to the Hankel functions and their derivatives. Since the frequency of interest here is 100 MHz or above, the phase $k_0 r$ in free space is $2\pi fr/c \geq 2\pi 100 \times 10^6 r/3 \times 10^8 = (2\pi/3)r$. As the transmitter-receiver distance r is at least the height of the vegetation layer height, i.e. $r \geq 20$ m, so that the condition $k_0 r \gg 1$ is always satisfied. Thus, the Hankel functions and derivatives used may be replaced by their asymptotic expressions. In addition, one over $D_3^{H,V}$ may be expressed in an infinite series form (binomial expansion).

For details of the field contributions, we separate the field into two parts E^x and E^z due to contributions of horizontal (x) and vertical (z) dipole moments, respectively, and waves associated with TE and TM modes. After exchanging the integration and the summation operations and using the complex transformation $\lambda = k_3 \sin\beta$, the field integrals may be written as

$$\begin{bmatrix} E^{>z}_{3z,TM} \\ E^{<z}_{3z,TM} \end{bmatrix} = -\frac{\omega\mu_o}{8\pi} P_z \sqrt{\frac{2k_3}{\pi\rho}} e^{-j\frac{\pi}{4}} \sum_{m=0}^{\infty} \begin{bmatrix} \mathcal{L}^{>}_{3z} \\ \mathcal{L}^{<}_{3z} \end{bmatrix}, \tag{8a}$$

$$\begin{bmatrix} E^{>x}_{3z,TM} \\ E^{<x}_{3z,TM} \end{bmatrix} = \frac{\omega\mu_o}{8\pi} P_x \cos\phi \sqrt{\frac{2k_3}{\pi\rho}} e^{-j\frac{\pi}{4}} \sum_{m=0}^{\infty} \begin{bmatrix} \mathcal{K}^{>}_{3z} \\ \mathcal{K}^{<}_{3z} \end{bmatrix}, \tag{8b}$$

$$\begin{bmatrix} E^{>z}_{3\rho,TM} \\ E^{<z}_{3\rho,TM} \end{bmatrix} = \mp\frac{\omega\mu_o}{8\pi} P_z \sqrt{\frac{2k_3}{\pi\rho}} e^{j\frac{3\pi}{4}} \sum_{m=0}^{\infty} \begin{bmatrix} \mathcal{L}^{>}_{3\rho} \\ \mathcal{L}^{<}_{3\rho} \end{bmatrix}, \tag{8c}$$

$$\begin{bmatrix} E^{>x}_{3\rho,TM} \\ E^{<x}_{3\rho,TM} \end{bmatrix} = -\frac{\omega\mu_o}{8\pi} P_x \cos\phi \sqrt{\frac{2k_3}{\pi\rho}} e^{-j\frac{\pi}{4}} \sum_{m=0}^{\infty} \begin{bmatrix} \mathcal{K}^{>}_{3\rho} \\ \mathcal{K}^{<}_{3\rho} \end{bmatrix}, \tag{8d}$$

$$\begin{bmatrix} E^{>x}_{3\rho,TE} \\ E^{<x}_{3\rho,TE} \end{bmatrix} = -\frac{\omega\mu_o}{8\pi\rho} P_x \cos\phi \sqrt{\frac{2}{\pi k_3\rho}} e^{-j\frac{3\pi}{4}} \sum_{m=0}^{\infty} \begin{bmatrix} \mathcal{G}^{>}_{3\rho} \\ \mathcal{G}^{<}_{3\rho} \end{bmatrix}, \tag{8e}$$

$$\begin{bmatrix} E^{>x}_{3\phi,TM} \\ E^{<x}_{3\phi,TM} \end{bmatrix} = \frac{\omega\mu_o}{8\pi\rho} P_x \sin\phi \sqrt{\frac{2}{\pi k_3\rho}} e^{-j\frac{3\pi}{4}} \sum_{m=0}^{\infty} \begin{bmatrix} \mathcal{K}^{>}_{3\phi} \\ \mathcal{K}^{<}_{3\phi} \end{bmatrix}, \tag{8f}$$

$$\begin{bmatrix} E^{>x}_{3\phi,TE} \\ E^{<x}_{3\phi,TE} \end{bmatrix} = \frac{\omega\mu_o}{8\pi} P_x \sin\phi \sqrt{\frac{2k_3}{\pi\rho}} e^{-j\frac{\pi}{4}} \sum_{m=0}^{\infty} \begin{bmatrix} \mathcal{G}^{>}_{3\phi} \\ \mathcal{G}^{<}_{3\phi} \end{bmatrix}, \tag{8g}$$

where the parameters in the integral domain are given by

$$\begin{bmatrix} \mathcal{L}_{3z}^{>} \\ \mathcal{L}_{3z}^{<} \end{bmatrix} = q_m \ \sin^{\frac{5}{2}}\beta \begin{bmatrix} \Phi_{-}^{>} \\ \Phi_{+}^{<} \end{bmatrix}, \tag{9a}$$

$$\begin{bmatrix} \mathcal{L}_{3\rho}^{>} \\ \mathcal{L}_{3\rho}^{<} \end{bmatrix} = q_m \ \sin^{\frac{3}{2}}\beta\cos\beta \begin{bmatrix} \Phi_{3\rho}^{>} \\ \Phi_{3\rho}^{<} \end{bmatrix}, \tag{9b}$$

$$\begin{bmatrix} \mathcal{K}_{3z}^{>} \\ \mathcal{K}_{3z}^{<} \end{bmatrix} = q_m \ \sin^{\frac{3}{2}}\beta\cos\beta \ \begin{bmatrix} \Phi_{+}^{>} \\ \Phi_{-}^{<} \end{bmatrix}, \tag{9c}$$

$$\begin{bmatrix} \mathcal{K}_{3\rho}^{>} \\ \mathcal{K}_{3\rho}^{<} \end{bmatrix} = q_m \ \sin^{\frac{1}{2}}\beta\cos^2\beta \begin{bmatrix} \Phi_{2\rho}^{>} \\ \Phi_{2\rho}^{<} \end{bmatrix}, \tag{9d}$$

$$\begin{bmatrix} \mathcal{K}_{3\phi}^{>} \\ \mathcal{K}_{3\phi}^{<} \end{bmatrix} = q_m \ \sin^{-\frac{1}{2}}\beta\cos^2\beta \begin{bmatrix} \Phi_{2\phi}^{>} \\ \Phi_{2\phi}^{<} \end{bmatrix}, \tag{9e}$$

$$\begin{bmatrix} \mathcal{G}_{3\rho}^{>} \\ \mathcal{G}_{3\rho}^{<} \end{bmatrix} = q'_m \ \sin^{-\frac{1}{2}}\beta \begin{bmatrix} \Phi_{1\rho}^{>} \\ \Phi_{1\rho}^{<} \end{bmatrix}, \tag{9f}$$

$$\begin{bmatrix} \mathcal{G}_{3\phi}^{>} \\ \mathcal{G}_{3\phi}^{<} \end{bmatrix} = q'_m \ \sin^{\frac{1}{2}}\beta \begin{bmatrix} \Phi_{1\phi}^{>} \\ \Phi_{1\phi}^{<} \end{bmatrix}, \tag{9g}$$

and

$$q_m = \int_{\Gamma_0} d\beta e^{jk_3\rho\sin\beta}(-1)^m \left[\left(R_2^V + R_1^V e^{j2H_1\sqrt{k_2^2-k_3^2\sin^2\beta}}\right)\right.$$
$$\left. R_3^V e^{j2H_2k_3\cos\beta} + R_1^V R_2^V e^{j2H_1\sqrt{k_2^2-k_3^2\sin^2\beta}}\right]^m, \tag{10a}$$

$$q'_m = \int_{\Gamma_0} d\beta e^{jk_3\rho\sin\beta}(-1)^m \left[\left(R_2^H + R_1^H e^{j2H_1\sqrt{k_2^2-k_3^2\sin^2\beta}}\right)\right.$$
$$\left. R_3^H e^{j2H_2k_3\cos\beta} + R_1^H R_2^H e^{j2H_1\sqrt{k_2^2-k_3^2\sin^2\beta}}\right]^m. \tag{10b}$$

To evaluate the integrals, the steepest descent method and the branch cut integration technique are used. For more information on the method, References [15] and [16] contain a good account of its meaning and application.

3.1 Direct and Multiple Reflected Waves

The integrals for the electromagnetic field components have been evaluated in this paper using the steepest descent method and hence expressed in terms of direct and multiple reflected waves. Following similar procedures as in [17] and [5], the saddle point part of the integrals have been evaluated and their solutions are given as (in the following, $*$ stands for $>$ or $<$):

$$
\begin{aligned}
E_{3z,TM}^{*z,s} = & -\frac{\omega\mu_0 P_z}{4\pi}\sqrt{\frac{k_3}{|k_3|}}e^{-j\frac{5\pi}{8}} \\
& \sum_{m=0}^{\infty} I_m^V \left\{ \left[1 + R_{1,s}^V(\beta_1^*)R_{2,s}^V(\beta_1^*)e^{bH_1}\right] a_1^* \right. \\
& \quad + \left[R_{2,s}^V(\beta_2^*) + R_{1,s}^V(\beta_2^*)e^{bH_1}\right] a_2^* \\
& \quad - R_{3,s}^V(\beta_3^*)\left[1 + R_{1,s}^V(\beta_3^*)R_{2,s}^V(\beta_3^*)e^{bH_1}\right] a_3^* \\
& \quad \left. - R_{3,s}^V(\beta_4^*)\left[R_{2,s}^V(\beta_4^*) + R_{1,s}^V(\beta_4^*)e^{bH_1}\right] a_4^* \right\},
\end{aligned} \tag{11a}
$$

$$
\begin{aligned}
E_{3z,TM}^{>x,s} = & \frac{\omega\mu_0}{4\pi}P_x\cos\phi\sqrt{\frac{k_3}{|k_3|}}e^{-j\frac{5\pi}{8}} \\
& \sum_{m=0}^{\infty} I_m^V \left\{ \left[1 + R_{1,s}^V(\beta_1^>)R_{2,s}^V(\beta_1^>)e^{bH_1}\right] \right. \\
& \quad \times a_1^> c_1^> + \left[R_{2,s}^V(\beta_2^>) + R_{1,s}^V(\beta_2^>)e^{bH_1}\right] a_2^> c_2^> \\
& \quad + R_{3,s}^V(\beta_3^>)\left[1 + R_{1,s}^V(\beta_3^>)R_{2,s}^V(\beta_3^>)e^{bH_1}\right] a_3^> c_3^> \\
& \quad \left. + R_{3,s}^V(\beta_4^>)\left[R_{2,s}^V(\beta_4^>) + R_{1,s}^V(\beta_4^>)e^{bH_1}\right] a_4^> c_4^> \right\},
\end{aligned} \tag{11b}
$$

$$
\begin{aligned}
E_{3z,TM}^{<x,s} = & \frac{\omega\mu_0}{4\pi}P_x\cos\phi\sqrt{\frac{k_3}{|k_3|}}e^{-j\frac{5\pi}{8}} \\
& \sum_{m=0}^{\infty} I_m^V \left\{ - \left[1 + R_{1,s}^V(\beta_1^<)R_{2,s}^V(\beta_1^<)e^{bH_1}\right] \right. \\
& \quad \times a_1^< c_1^< + \left[R_{2,s}^V(\beta_2^<) + R_{1,s}^V(\beta_2^<)e^{bH_1}\right] a_2^< c_2^< \\
& \quad + R_{3,s}^V(\beta_3^<)\left[1 + R_{1,s}^V(\beta_3^<)R_{2,s}^V(\beta_3^<)e^{bH_1}\right] a_3^< c_3^< \\
& \quad \left. - R_{3,s}^V(\beta_4^<)\left[R_{2,s}^V(\beta_4^<) + R_{1,s}^V(\beta_4^<)e^{bH_1}\right] a_4^< c_4^< \right\},
\end{aligned} \tag{11c}
$$

$$
\begin{aligned}
E_{3\rho,TM}^{>z,s} = & -\frac{\omega\mu_o}{4\pi}P_z\sqrt{\frac{k_3}{|k_3|}}e^{\frac{3\pi}{8}} \\
& \sum_{m=0}^{\infty} I_m^V \left\{ \left[1 + R_{1,s}^V(\beta_1^>)R_{2,s}^V(\beta_1^>)e^{bH_1}\right] a_1^> e_1^> \right.
\end{aligned}
$$

$$
\begin{aligned}
& - \left[R^V_{2,s}(\beta^>_2) + R^V_{1,s}(\beta^>_2) e^{bH_1} \right] a^>_2 e^>_2 \\
& - R^V_{3,s}(\beta^>_3) \left[1 + R^V_{1,s}(\beta^>_3) R^V_{2,s}(\beta^>_3) e^{bH_1} \right] a^>_3 e^>_3 \\
& + R^V_{3,s}(\beta^>_4) \left[R^V_{2,s}(\beta^>_4) + R^V_{1,s}(\beta^>_4) e^{bH_1} \right] a^>_4 e^>_4 \Big\}, \qquad \text{(11d)}
\end{aligned}
$$

$$
\begin{aligned}
E^{<z,s}_{3\rho,TM} = & \frac{\omega\mu_o}{4\pi} P_z \sqrt{\frac{k_3}{|k_3|}} e^{\frac{3\pi}{8}} \\
& \sum_{m=0}^{\infty} I^V_m \Big\{ \left[1 + R^V_{1,s}(\beta^<_1) R^V_{2,s}(\beta^<_1) e^{bH_1} \right] a^<_1 e^<_1 \\
& + \left[R^V_{2,s}(\beta^<_2) + R^V_{1,s}(\beta^<_2) e^{bH_1} \right] a^<_2 e^<_2 \\
& + R^V_{3,s}(\beta^<_3) \left[1 + R^V_{1,s}(\beta^<_3) R^V_{2,s}(\beta^<_3) e^{bH_1} \right] a^<_3 e^<_3 \\
& + R^V_{3,s}(\beta^<_4) \left[R^V_{2,s}(\beta^<_4) + R^V_{1,s}(\beta^<_4) e^{bH_1} \right] a^<_4 e^<_4 \Big\}, \qquad \text{(11e)}
\end{aligned}
$$

$$
\begin{aligned}
E^{*x,s}_{3\rho,TM} = & -\frac{\omega\mu_o}{4\pi} P_x \cos\phi \sqrt{\frac{k_3}{|k_3|}} e^{-\frac{5\pi}{8}} \\
& \sum_{m=0}^{\infty} I^V_m \Big\{ \left[1 + R^V_{1,s}(\beta^*_1) R^V_{2,s}(\beta^*_1) e^{bH_1} \right] \\
& \times a^*_1 f^*_1 - \left[R^V_{2,s}(\beta^*_2) + R^V_{1,s}(\beta^*_2) e^{bH_1} \right] a^*_2 f^*_2 \\
& + R^V_{3,s}(\beta^*_3) \left[1 + R^V_{1,s}(\beta^*_3) R^V_{2,s}(\beta^*_3) e^{bH_1} \right] a^*_3 f^*_3 \\
& - R^V_{3,s}(\beta^*_4) \left[R^V_{2,s}(\beta^*_4) + R^V_{1,s}(\beta^*_4) e^{bH_1} \right] a^*_4 f^*_4 \Big\}, \qquad \text{(11f)}
\end{aligned}
$$

$$
\begin{aligned}
E^{*x,s}_{3\rho,TE} = & -\frac{\omega\mu_o}{4\pi\rho} P_x \cos\phi \frac{e^{-\frac{9\pi}{8}}}{\sqrt{k_3|k_3|}} \\
& \sum_{m=0}^{\infty} I^H_m \Big\{ \left[1 + R^H_{1,s}(\beta^*_1) R^H_{2,s}(\beta^*_1) e^{bH_1} \right] a^*_1 \\
& + \left[R^H_{2,s}(\beta^*_2) + R^H_{1,s}(\beta^*_2) e^{bH_1} \right] a^*_2 \\
& - R^H_{3,s}(\beta^*_3) \left[1 + R^H_{1,s}(\beta^*_3) R^H_{2,s}(\beta^*_3) e^{bH_1} \right] a^*_3 \\
& - R^H_{3,s}(\beta^*_4) \left[R^H_{2,s}(\beta^*_4) + R^H_{1,s}(\beta^*_4) e^{bH_1} \right] a^*_4 \Big\}, \qquad \text{(11g)}
\end{aligned}
$$

$$
\begin{aligned}
E^{*x,s}_{3\phi,TM} = & \frac{\omega\mu_o}{4\pi\rho} P_x \sin\phi \frac{e^{-\frac{9\pi}{8}}}{\sqrt{k_3|k_3|}} \\
& \sum_{m=0}^{\infty} I^V_m \left\{ \left[1 + R^V_{1,s}(\beta^*_1) R^V_{2,s}(\beta^*_1) e^{bH_1}\right] a^*_1 g^*_1 \right. \\
& \quad - \left[R^V_{2,s}(\beta^*_2) + R^V_{1,s}(\beta^*_2) e^{bH_1}\right] a^*_2 g^*_2 \\
& \quad + R^V_{3,s}(\beta^*_3) \left[1 + R^V_{1,s}(\beta^*_3) R^V_{2,s}(\beta^*_3) e^{bH_1}\right] a^*_3 g^*_3 \\
& \quad \left. - R^V_{3,s}(\beta^*_4) \left[R^V_{2,s}(\beta^*_4) + R^V_{1,s}(\beta^*_4) e^{bH_1}\right] a^*_4 g^*_4 \right\}, \qquad \text{(11h)}
\end{aligned}
$$

$$
\begin{aligned}
E^{*x,s}_{3\phi,TE} = & \frac{\omega\mu_o}{4\pi} P_x \sin\phi \sqrt{\frac{k_3}{|k_3|}} e^{-\frac{5\pi}{8}} \\
& \sum_{m=0}^{\infty} I^H_m \left\{ \left[1 + R^H_{1,s}(\beta^*_1) R^H_{2,s}(\beta^*_1) e^{bH_1}\right] a^*_1 \right. \\
& + \left[R^H_{2,s}(\beta^*_2) + R^H_{1,s}(\beta^*_2) e^{bH_1}\right] a^*_2 \\
& - R^H_{3,s}(\beta^*_3) \left[1 + R^H_{1,s}(\beta^*_3) R^H_{2,s}(\beta^*_3) e^{bH_1}\right] a^*_3 \\
& \left. - R^H_{3,s}(\beta^*_4) \left[R^H_{2,s}(\beta^*_4) + R^H_{1,s}(\beta^*_4) e^{bH_1}\right] a^*_4 \right\}, \qquad \text{(11i)}
\end{aligned}
$$

where the intermediate parameters such as θ^*_ℓ , β^*_ℓ $R^{H,V}_{\ell,s}$, a^*_ℓ , b , c^*_ℓ , $d^*_\pm$, e^*_ℓ , f^*_ℓ , and g^*_ℓ have been given in the Appendix.

3.2 Lateral Waves

The solutions of the integrals in (8b)–(8g) can be evaluated using the residue theorem in a way similar to that available in the literature [17], [15] and [16]. Correspondingly, the branch cut contributions of $h_2 = 0$ and $h_4 = 0$ to the fields have been obtained, respectively. The lateral waves along three different ways namely, the lateral waves at the air-canopy interface, at the canopy-trunk interface, and at the trunk-ground interface have been from the analysis. The mixed modes propagation mechanisms of radio waves in the trunk layer radiated by a dipole antenna located inside the trunk layer have been clearly shown in Fig. 2. For the cases that are considered here, while the lateral waves along the second and third interfaces are highly attenuated due to the

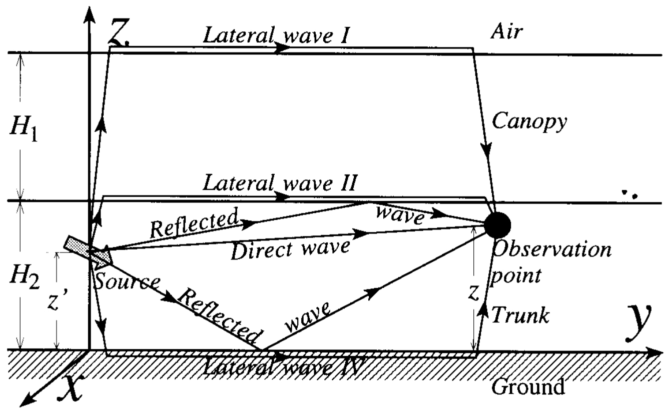

Figure 2. Mixed mode propagation of the radio waves radiated by a dipole antenna located inside the forest trunk layer.

high conductivity of canopy and ground media, the lateral wave at the air-canopy interface is propagating primarily in a lossless medium.

3.2.1 Along the air-canopy interface

Using the parameters given in the appendix, the branch cut contribution due to branch point h_1, which is equivalent to lateral wave along the air-canopy interface, can be expressed as

$$\mathcal{L}_{3z}^{>c1} = -j2n_2^2 n_1 \sqrt{\frac{2\pi(1-n_1^2)^{1/2}}{n_2^2-n_1^2}} e^{-j\frac{\pi}{4}} \frac{e^{jb_1}}{b_2^{3/2}} (-1)^m \Gamma_1 d_1^m \left[a_1 + \frac{mc_1 d_2}{d_1}\right], \tag{12a}$$

$$\mathcal{K}_{3z}^{>c1} = \frac{\sqrt{1-n_1^2}}{n_1} \frac{\Gamma_2}{\Gamma_1} \mathcal{L}_{3z}^{>,c1}, \tag{12b}$$

$$\mathcal{L}_{3\rho}^{>c1} = -j2n_2^2 \sqrt{\frac{2\pi}{n_2^2-n_1^2}} (1-n_1^2)^{\frac{3}{4}} e^{-j\frac{\pi}{4}} \frac{e^{jb_1}}{b_2^{3/2}} (-1)^m \Gamma_1 d_1^m \left[a_2 + \frac{mc_1 d_3}{d_1}\right], \tag{12c}$$

$$\mathcal{K}_{3\rho}^{>c1} = \frac{\sqrt{1-n_1^2}}{n_1} \frac{\Gamma_2}{\Gamma_1} \mathcal{L}_{3\rho}^{>c1}, \tag{12d}$$

$$\mathcal{G}_{3\rho}^{>c1} = j2 \sqrt{\frac{2\pi(1-n_1^2)^{1/2}}{n_2^2-n_1^2}} e^{-j\frac{\pi}{4}} \frac{e^{jb_1}}{b_2^{3/2}} (-1)^m \Gamma_3 d_4^m \left[a_3 + \frac{mc_2 d_5}{d_4}\right], \tag{12e}$$

$$\mathcal{K}_{3\phi}^{>c1} = \frac{1}{n_1}\mathcal{K}_{3\rho}^{>c1}, \tag{12f}$$

$$\mathcal{G}_{3\phi}^{>c1} = n_1\mathcal{G}_{3\rho}^{>c1}, \tag{12g}$$

and

$$\mathcal{K}_{3z}^{<c1} = -j2n_2^2\sqrt{\frac{2\pi(1-n_1^2)^{3/2}}{n_2^2-n_1^2}}e^{-j\frac{\pi}{4}}\frac{e^{jb_1}}{b_2^{3/2}}(-1)^m\Gamma_4 d_1^m\left[a_4+\frac{mc_1d_6}{d_1}\right], \tag{13a}$$

$$\mathcal{L}_{3\rho}^{<c1} = -j2n_2^2\sqrt{\frac{2\pi}{n_2^2-n_1^2}}(1-n_1^2)^{\frac{3}{4}}e^{-j\frac{\pi}{4}}\frac{e^{jb_1}}{b_2^{3/2}}(-1)^m\Gamma_5 d_1^m\left[a_5+\frac{mc_1d_7}{d_1}\right], \tag{13b}$$

and the expressions for $\mathcal{L}_{3z}^{<cl}$, $\mathcal{K}_{3\rho}^{<c1}$, $\mathcal{G}_{3\rho}^{<c1}$, $\mathcal{K}_{3\phi}^{<c1}$, and $\mathcal{G}_{3\phi}^{<c1}$ are given by (12a), (12d), (12e), (12f), and (12g) respectively, with the positions of z and z' interchanged.

Similar procedures can be employed to obtain the branch cut contributions due to h_2 and h_4, which accounts for the lateral waves at canopy-trunk interface, and trunk-ground interface. The complete solutions of the lateral waves along the two interfaces are presented below.

3.2.2 Along the canopy-trunk interface

Using the parameters given in the appendix,

$$\mathcal{L}_{3z}^{>c2} = j2n_2\sqrt{2\pi}e^{-j\frac{\pi}{4}}\frac{e^{jb_1}}{b_2^{3/2}}\,\Gamma_1\,e^{-j2mh_3H_2} \times\left[\frac{n_1^2(1-n_2^2)^{1/4}}{\sqrt{n_1^2-n_2^2}}a_1-(1-n_2^2)^{-1/4}a_2\right], \tag{14a}$$

$$\mathcal{K}_{3z}^{>c2} = \frac{\sqrt{1-n_2^2}}{n_2}\frac{\Gamma_2}{\Gamma_1}\mathcal{L}_{3z}^{>c2}, \tag{14b}$$

$$\mathcal{L}_{3\rho}^{>c2} = -j2\sqrt{2\pi(1-n_2^2)}e^{-j\frac{\pi}{4}}\frac{e^{jb_1}}{b_2^{3/2}}\,\Gamma_1\,e^{-j2mh_3H_2} \times\left[\frac{-a_1}{(1-n_2^2)^{\frac{1}{4}}}+a_2n_1^2\sqrt{\frac{(1-n_2^2)^{1/2}}{n_1^2-n_2^2}}\right], \tag{14c}$$

$$\mathcal{K}_{3\rho}^{>c2} = \frac{\sqrt{1-n_2^2}}{n_2}\frac{\Gamma_2}{\Gamma_1}\mathcal{L}_{3\rho}^{>c2}, \tag{14d}$$

$$\mathcal{G}_{3\rho}^{>c2} = -j2\sqrt{2\pi}(1-n_2^2)^{\frac{1}{4}}e^{-j\frac{\pi}{4}}\frac{e^{jb_1}}{b_2^{3/2}}\;\Gamma_3\;e^{-j2mh_3H_2} \times\left[\frac{a_2}{\sqrt{n_1^2-n_2^2}}-\frac{a_1}{\sqrt{n_3^2-n_2^2}}\right], \tag{14e}$$

$$\mathcal{K}_{3\phi}^{>c2} = \frac{1}{n_2}\mathcal{K}_{3\rho}^{>c2}, \tag{14f}$$

$$\mathcal{G}_{3\phi}^{>c2} = n_2\mathcal{G}_{3\rho}^{>c2}, \tag{14g}$$

and

$$\mathcal{K}_{3z}^{<c2} = j2n_2\frac{\sqrt{1-n_2^2}}{n_2}\sqrt{2\pi}e^{-j\frac{\pi}{4}}\frac{e^{jb_1}}{b_2^{3/2}}\;\Gamma_4\;e^{-j2mh_3H_2} \times\left[\frac{n_1^2(1-n_2^2)^{1/4}}{\sqrt{n_1^2-n_2^2}}a_4-(1-n_2^2)^{-1/4}a_3\right], \tag{15a}$$

$$\mathcal{L}_{3\rho}^{<c2} = -j2\sqrt{2\pi(1-n_2^2)}e^{-j\frac{\pi}{4}}\frac{e^{jb_1}}{b_2^{3/2}}\;\Gamma_5\;e^{-j2mh_3H_2} \times\left[\frac{a_4}{(1-n_2^2)^{\frac{1}{4}}}-a_3n_1^2\sqrt{\frac{(1-n_2^2)^{1/2}}{n_1^2-n_2^2}}\right], \tag{15b}$$

and the expressions for $\mathcal{L}_{3z}^{<c2}$, $\mathcal{K}_{3\rho}^{<c2}$, $\mathcal{G}_{3\rho}^{<c2}$, $\mathcal{K}_{3\phi}^{<c2}$, and $\mathcal{G}_{3\phi}^{<c2}$ are given by (14a), (14d), (14e), (14f), and (14g) respectively, with the positions of z and z' interchanged.

3.2.1 Along the trunk-ground interface

Again, using the parameters give in appendix,

$$\mathcal{L}_{3z}^{>c4} = j2n_4\sqrt{\frac{2\pi}{(1-n_4^2)^{1/2}}}e^{-j\frac{\pi}{4}}\frac{e^{jb_1}}{b_2^{3/2}}(-1)^m\;\Gamma_1a_3^m\left[a_1+\frac{mc_1a_2}{a_3}\right],$$

$$\tag{16a}$$

$$\mathcal{K}_{3z}^{>c4} = \frac{\sqrt{1-n_4^2}}{n_4}\mathcal{L}_{3z}^{>c4} \quad \text{with} \quad a_1 = e^{j2h_3z'}, \tag{16b}$$

$$\mathcal{L}_{3\rho}^{>c4} = j2\sqrt{2\pi}(1-n_4^2)^{\frac{1}{4}}e^{-j\frac{\pi}{4}}\frac{e^{jb_1}}{b_2^{3/2}}(-1)^m\,\Gamma_2 a_3^m\left[a_1+\frac{mc_1a_2}{a_3}\right], \tag{16c}$$

$$\mathcal{K}_{3\rho}^{>c4} = \frac{\sqrt{1-n_4^2}}{n_4}\mathcal{L}_{3\rho}^{>c4} \quad \text{with} \quad a_1 = e^{j2h_3z'}, \tag{16d}$$

$$\mathcal{G}_{3\rho}^{>c4} = -j2\sqrt{\frac{2\pi}{(1-n_4^2)^{\frac{1}{2}}}}e^{-j\frac{\pi}{4}}\frac{e^{jb_1}}{b_2^{3/2}}(-1)^m\,\Gamma_3 a_5^m\left[a_1+\frac{mc_2a_4}{a_5}\right], \tag{16e}$$

$$\mathcal{K}_{3\phi}^{>c4} = \frac{1}{n_4}\mathcal{K}_{3\rho}^{>c4}, \tag{16f}$$

$$\mathcal{G}_{3\phi}^{>c4} = n_4\mathcal{G}_{3\rho}^{>c4}, \tag{16g}$$

and

$$\mathcal{K}_{3z}^{<c4} = j2\sqrt{2\pi(1-n_4^2)^{1/2}}e^{-j\frac{\pi}{4}}\frac{e^{jb_1}}{b_2^{3/2}}(-1)^m\,\Gamma_4 a_3^m\left[a_6+\frac{mc_1a_7}{a_3}\right], \tag{17a}$$

$$\mathcal{L}_{3\rho}^{<c4} = j2\sqrt{2\pi}(1-n_4^2)^{\frac{1}{4}}e^{-j\frac{\pi}{4}}\frac{e^{jb_1}}{b_2^{3/2}}(-1)^m\,\Gamma_5 a_3^m\left[a_8+\frac{mc_1a_9}{a_3}\right]. \tag{17b}$$

Expressions for $\mathcal{L}_{3z}^{<c4}$, $\mathcal{K}_{3\rho}^{<c4}$, $\mathcal{G}_{3\rho}^{<c4}$, $\mathcal{K}_{3\phi}^{<c4}$, and $\mathcal{G}_{3\phi}^{<c4}$ used as above are given by (16a), (16d), (16e), (16f), and (16g), respectively, with the positions of z and z' interchanged. This concludes the analysis of all the radio waves propagating in such a four-layered medium.

4. RESULTS AND DISCUSSION

The forest model described can be employed to estimate or predict the performance of communication systems operating within forested environment. This section looks at the transmission loss when the transmitter and the receiver are both located in the same layer (trunk). The radio loss L from an inclined dipole to a vertical receiving antenna is given by [1]

$$L(\mathrm{dB}) = 36.57 + 20\log_{10} f + 20\log_{10}|E_o| - 20\log_{10}|E| \tag{18}$$

where f is the frequency in GHz and E_o is the reference field in the absence of the forest given by

$$|E_o| = \frac{\omega\mu_o}{4\pi}\sqrt{\frac{P_x^2 + P_z^2}{\rho^2 + (z - z')^2}}. \tag{19}$$

Having obtained all the different components of the electric field, we can find the total overall electric field which is given by

$$|E_{3,\ \mathrm{total}}|^2 = |E_{3z}|^2 + |E_{3\rho}|^2 + |E_{3\phi}|^2. \tag{20}$$

It should be pointed out that the optimum angle obtained in [5] is not correct. It is simply because there is a constant factor missing in the presentation of the electric field z-component. If we consider the total contribution of all the components as given in (20), the expression of the optimum angle in [5] is also incorrect.

For a tropical 'dense' forest, the ground has a relative permittivity $\epsilon_r = 50$ and conductivity $\sigma = 0.1$ S/m, the canopy medium has relative permittivity $\epsilon_r = 40$ and conductivity $\sigma = 0.0003$ S/m, and the trunk medium has a relative permittivity $\epsilon_r = 35$ and conductivity $\sigma = 0.0001$ S/m. The transmitter is located at a height of 10 m and the receiver at a height of 15 m. Heights of trunk and canopy layers are typically 10 and 20 m, respectively.

Using these parameters for the forest, transmission loss has been computed for different orientations of the dipole transmitter and various frequencies, and depicted subsequently from Fig. 3 to Fig. 8.

The path losses for the vertical, horizontal and 45° inclined dipoles are shown in Fig. 3 as functions of the distance between transmitter and receiver at 500 MHz, along the x-direction. As observed, direct and multiple reflected waves dominate the field at near zone. Lateral waves become, however, the dominant radio wave propagation mechanism when the distance increases. Transmission attenuation saturates at large distances since propagation is dominated by lateral wave along the lossless air medium at the air-canopy interface. Above 4 km at this frequency, electric field is primarily determined from the lateral wave. For our case, overall electric field from a horizontal dipole suffers less

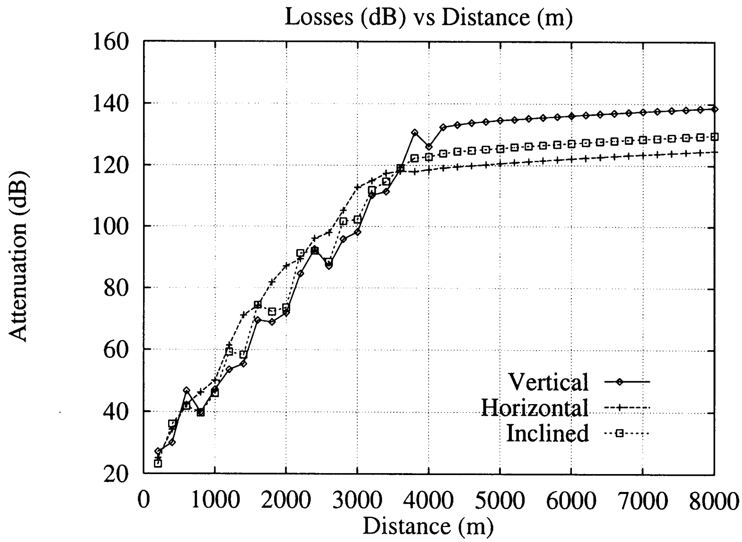

Figure 3. Attenuation of total electric field due to a dipole with different orientations in the trunk layer at 500 MHz and $\phi = 0°$.

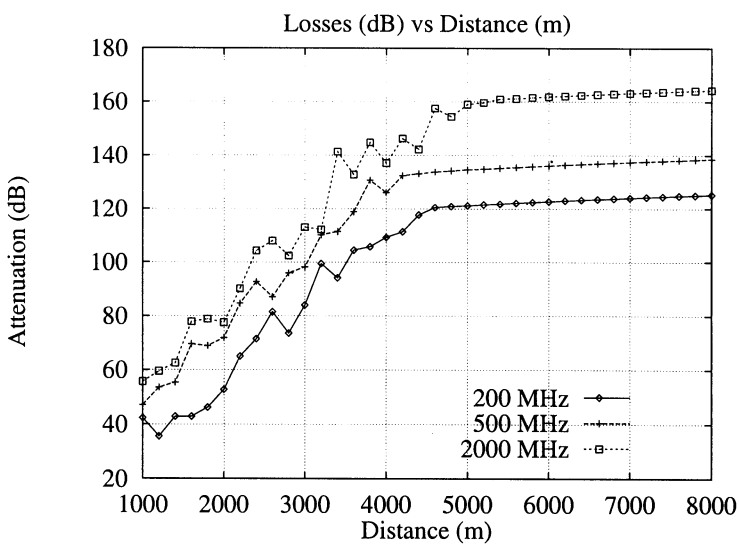

Figure 4. Attenuation of total electric field due to a vertical dipole in the trunk layer.

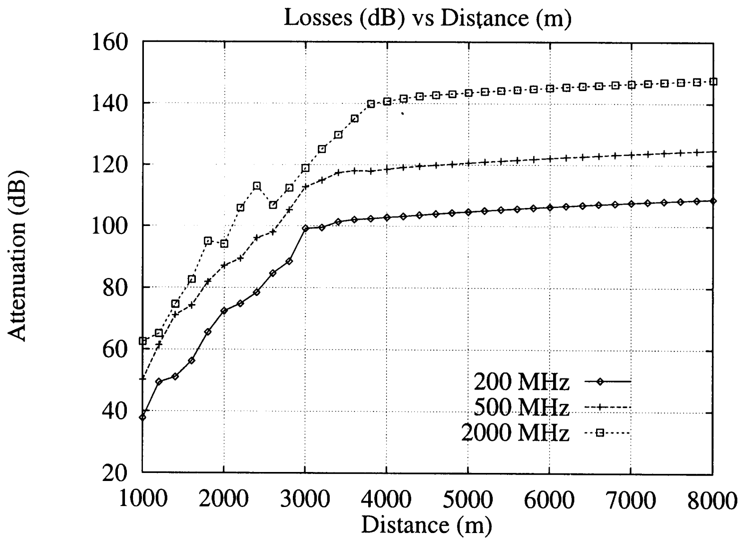

Figure 5. Attenuation of total electric field due to a horizontal dipole in the trunk layer at $\phi = 0°$.

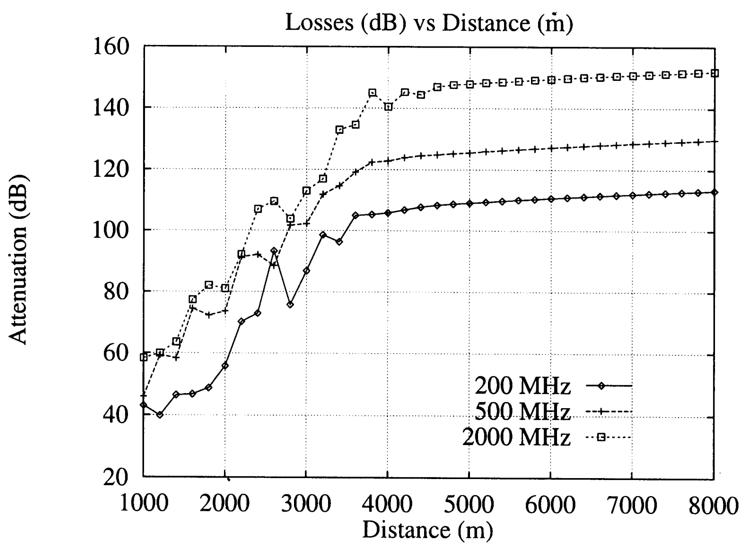

Figure 6. Attenuation of total electric field due to a 45° inclined dipole in the trunk layer at $\phi = 0°$.

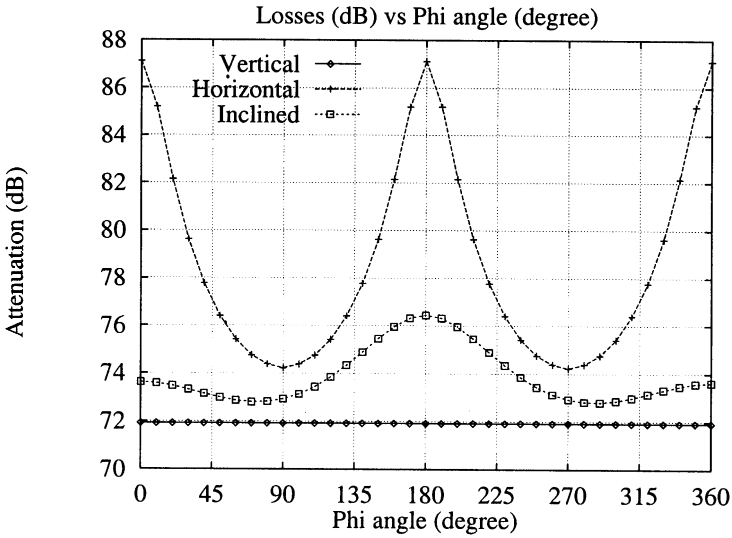

Figure 7. Attenuation of total electric field at 500 MHz and $\rho = 2\ km$.

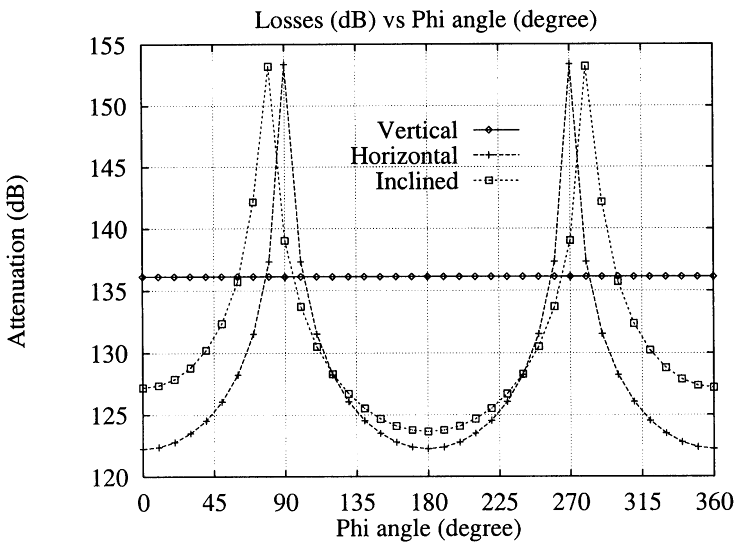

Figure 8. Attenuation of total electric field at 500 MHz and $\rho = 6\ km$.

attenuation as compared to that from a vertical dipole, about 14 dB lesser. It is also observed from Fig. 3 that, for given conditions the radio wave due to a horizontal dipole has least attenuation in the far zone and most transmission loss in the near zone as compared to the other orientations, and certainly the wave due to a vertical dipole has the inverse conclusion.

The effect of frequency on the transmission loss experienced by the radio wave propagation in the presence of forest is shown in Figs. 4, 5 and 6. As frequency increases, there is a trend of increasing attenuation for all three orientation of dipoles considered here. In the near zone (from 0 to 4 km without respect to the wavelength), the speed of such a attenuation increase is much higher than that in the far zone (from 4 km to 8 km or above).

The effect of varying the position of the receiver in the cylindrical angle, ϕ on the attenuation experienced by the electric field is shown in Figs. 7 and 8. Apparently, the field is not isotropic with respect to the polar angle ϕ, but periodic instead. For field dominated by direct and multiple reflected wave, received overall field suffers least attenuation at 90° from horizontal dipole, and at around 70° from dipole with a 45° inclination. For lateral wave dominated field, least attenuation occurs at 180° for both horizontal and inclined dipoles.

5. CONCLUSIONS

In this paper, the propagation of electromagnetic waves in a medium with four horizontal layers has been studied using dyadic Green's functions. This method presents some advantages as (i) the dyadic Green's functions outside the source region allow a higher degree of flexibility with respect to the space coordinates and assure a good exponential convergence; (ii) the source may contain an arbitrary current distribution; and (iii) the medium may be isotropic or anisotropic. The exact integral solution of the electric field due to an electric dipole of an arbitrarily inclination has been obtained. The asymptotic expressions of *all the electric field components* are further obtained by the use of the saddle point technique and the branch cut integrations. Correspondingly, three types of waves, i.e., the direct wave, the (multi-)reflected waves, and lateral waves, have been represented in their closed forms. The transmission losses of these waves have been computed numerically and compared each other. It is found that the only the lateral wave propagating along the upper air-canopy interface dominates the total field in the far zone while the direct wave together with reflected waves of several hops play an important role in the total field in the quite near zone. The results presented in this paper give an insight into the behavior of the electromagnetic waves due to an inclined dipole located in the trunk layer and into the mechanism of the mixed mode propagation of the waves in such a four-layered forest model.

APPENDIX. FORMULAS USED IN THE ANALYSIS

Note that there is a repetition of the parameters used in the analysis of the saddle point part and lateral wave contributions of the field.

A.1 Direct and Multiple Reflected Waves

Ray-path distances are given by:

$$r_{\pm}^{>} = \sqrt{\rho^2 + (2mH_2 + z \pm z')^2}, \tag{21a}$$

$$r_{\pm}'^{>} = \sqrt{\rho^2 + [2(m+1)H_2 - z \pm z']^2}, \tag{21b}$$

$$r_{\pm}^{<} = \sqrt{\rho^2 + (2mH_2 + z' \pm z)^2}, \tag{21c}$$

$$r_{\pm}'^{<} = \sqrt{\rho^2 + [2(m+1)H_2 - z' \pm z]^2}. \tag{21d}$$

Angles of incidence, β_ℓ ($\ell = 1, 2, 3, 4$), and angles of total internal reflection, θ_ℓ ($\ell = 1, 2, 3, 4$) are listed by:

$$\theta_1^{>} = \sin^{-1}\left(\frac{2mH_2 + z - z'}{r_-^{>}}\right), \tag{22a}$$

$$\theta_2^{>} = \sin^{-1}\left(\frac{2(m+1)H_2 - z - z'}{r_-'^{>}}\right), \tag{22b}$$

$$\theta_3^{>} = \sin^{-1}\left(\frac{2mH_2 + z + z'}{r_+^{>}}\right), \tag{22c}$$

$$\theta_4^{>} = \sin^{-1}\left(\frac{2(m+1)H_2 - z + z'}{r_+'^{>}}\right), \tag{22d}$$

$$\theta_1^{<} = \sin^{-1}\left(\frac{2mH_2 + z' - z}{r_-^{<}}\right), \tag{22e}$$

$$\theta_2^{<} = \sin^{-1}\left(\frac{2(m+1)H_2 - z' - z}{r_-'^{<}}\right), \tag{22f}$$

$$\theta_3^< = \sin^{-1}\left(\frac{2mH_2 + z' + z}{r_+^<}\right), \tag{22g}$$

$$\theta_4^< = \sin^{-1}\left(\frac{2(m+1)H_2 - z' + z}{r_+'^<}\right), \tag{22h}$$

$$\beta_1^> = \frac{\pi}{2} - \theta_1^>, \quad \beta_2^> = \frac{\pi}{2} - \theta_2^>, \quad \beta_3^> = \frac{\pi}{2} - \theta_3^>, \quad \beta_4^> = \frac{\pi}{2} - \theta_4^>, \tag{22i}$$

$$\beta_1^< = \frac{\pi}{2} - \theta_1^<, \quad \beta_2^< = \frac{\pi}{2} - \theta_2^<, \quad \beta_3^< = \frac{\pi}{2} - \theta_3^<, \quad \beta_4^< = \frac{\pi}{2} - \theta_4^<. \tag{22j}$$

Reflection coefficients at the interfaces ($i = 1$, 2, 3 and 4, and again $*$ denotes $<$ or $>$) are:

$$R_{1,s}^V(\beta_i^*) = \frac{k_2^2\sqrt{k_1^2 - k_3^2\sin^2\beta_i^*} - k_1^2\sqrt{k_2^2 - k_3^2\sin^2\beta_i^*}}{k_2^2\sqrt{k_1^2 - k_3^2\sin^2\beta_i^*} + k_1^2\sqrt{k_2^2 - k_3^2\sin^2\beta_i^*}}, \tag{23a}$$

$$R_{2,s}^V(\beta_i^*) = \frac{k_3^2\sqrt{k_2^2 - k_3^2\sin^2\beta_i^*} - k_2^2 k_3\cos\beta_i^*}{k_3^2\sqrt{k_2^2 - k_3^2\sin^2\beta_i^*} + k_2^2 k_3\cos\beta_i^*}, \tag{23b}$$

$$R_{3,s}^V(\beta_i^*) = \frac{k_4^2 k_3\cos\beta_i^* - k_3^2\sqrt{k_4^2 - k_3^2\sin^2\beta_i^*}}{k_4^2 k_3\cos\beta_i^* + k_3^2\sqrt{k_4^2 - k_3^2\sin^2\beta_i^*}}, \tag{23c}$$

$$R_{1,s}^H(\beta_i^*) = \frac{\sqrt{k_2^2 - k_3^2\sin^2\beta_i^*} - \sqrt{k_1^2 - k_3^2\sin^2\beta_i^*}}{\sqrt{k_2^2 - k_3^2\sin^2\beta_i^*} + \sqrt{k_1^2 - k_3^2\sin^2\beta_i^*}}, \tag{23d}$$

$$R_{2,s}^H(\beta_i^*) = \frac{k_3\cos\beta_i^* - \sqrt{k_2^2 - k_3^2\sin^2\beta_i^*}}{k_3\cos\beta_i^* + \sqrt{k_2^2 - k_3^2\sin^2\beta_i^*}}, \tag{23e}$$

$$R_{3,s}^H(\beta_i^*) = \frac{\sqrt{k_4^2 - k_3^2\sin^2\beta_i^*} - k_3\cos\beta_i^*}{\sqrt{k_4^2 - k_3^2\sin^2\beta_i^*} + k_3\cos\beta_i^*}. \tag{23f}$$

Substituted parameters (where $*$ stands for either $<$ or $>$) are given as follows:

$$I_m^{H,V} = \Big[R_{3,s}^{H,V}\big(R_{2,s}^{H,V} + R_{1,s}^{H,V} e^{j2H_1\sqrt{k_2^2 - k_3^2}}\big)$$

$$+R_{1,s}^{H,V} R_{2,s}^{H,V} e^{j2H_1\sqrt{k_2^2-k_3^2}}\Big]^m (-1)^m, \tag{24a}$$

$$a_1^* = \frac{e^{jk_3 r_-^*}}{\sqrt{\rho r_-^*}}, \quad a_2^* = \frac{e^{jk_3 r_-^{'*}}}{\sqrt{\rho r_-^{'*}}}, \quad a_3^* = \frac{e^{jk_3 r_+^*}}{\sqrt{\rho r_+^*}}, \quad a_4^* = \frac{e^{jk_3 r_+^{'*}}}{\sqrt{\rho r_+^{'*}}}, \tag{24b}$$

$$b = j2\sqrt{k_2^2 - k_3^2}, \tag{24c}$$

$$c_1^* = \frac{|d_-^*|}{\rho}, \quad c_2^* = \frac{|d_-^{'*}|}{\rho}, \quad c_3^* = \frac{|d_+^*|}{\rho}, \quad c_4^* = \frac{|d_+^{'*}|}{\rho}, \tag{24d}$$

$$e_1^* = \frac{\rho^2|d_-^*|}{(r_-^*)^3}, \quad e_2^* = \frac{\rho^2|d_-^{'*}|}{(r_-^{'*})^3}, \quad e_3^* = \frac{\rho^2|d_+^*|}{(r_+^*)^3}, \quad e_4^* = \frac{\rho^2|d_+^{'*}|}{(r_+^{'*})^3}, \tag{24e}$$

$$f_1^* = \frac{\rho(d_-^*)^2}{(r_-^*)^3}, \quad f_2^* = \frac{\rho(d_-^{'*})^2}{(r_-^{'*})^3}, \quad f_3^* = \frac{\rho(d_+^*)^2}{(r_+^*)^3}, \quad f_4^* = \frac{\rho(d_+^{'*})^2}{(r_+^{'*})^3}, \tag{24f}$$

$$g_1^* = \frac{(d_-^*)^2}{\rho r_-^*}, \quad g_2^* = \frac{(d_-^{'*})^2}{\rho r_-^{'*}}, \quad g_3^* = \frac{(d_+^*)^2}{\rho r_+^*}, \quad g_4^* = \frac{(d_+^{'*})^2}{\rho r_+^{'*}}, \tag{24g}$$

where

$$d_\pm^> = 2mH_2 + z \pm z', \tag{25a}$$

$$d_\pm^{'>} = 2(m+1)H_2 - z \pm z', \tag{25b}$$

$$d_\pm^< = 2mH_2 + z' \pm z, \tag{25c}$$

$$d_\pm^{'<} = 2(m+1)H_2 - z' \pm z. \tag{25d}$$

A.2 Lateral Wave

Reflection coefficients at interfaces are provided by:

$$R_{2,c1}^H = \frac{\sqrt{k_3^2 - k_1^2} - \sqrt{k_2^2 - k_1^2}}{\sqrt{k_3^2 - k_1^2} + \sqrt{k_2^2 - k_1^2}}, \tag{26a}$$

$$R_{3,c1}^H = \frac{\sqrt{k_4^2 - k_1^2} - \sqrt{k_3^2 - k_1^2}}{\sqrt{k_4^2 - k_1^2} + \sqrt{k_3^2 - k_1^2}}, \tag{26b}$$

$$R_{2,c1}^V = \frac{k_3^2\sqrt{k_2^2 - k_1^2} - k_2^2\sqrt{k_3^2 - k_1^2}}{k_3^2\sqrt{k_2^2 - k_1^2} + k_2^2\sqrt{k_3^2 - k_1^2}}, \tag{26c}$$

$$R_{3,c1}^V = \frac{k_4^2\sqrt{k_3^2 - k_1^2} - k_3^2\sqrt{k_4^2 - k_1^2}}{k_4^2\sqrt{k_3^2 - k_1^2} + k_3^2\sqrt{k_4^2 - k_1^2}}, \tag{26d}$$

$$R_{3,c2}^{H} = \frac{\sqrt{k_4^2 - k_2^2} - \sqrt{k_3^2 - k_2^2}}{\sqrt{k_4^2 - k_2^2} + \sqrt{k_3^2 - k_2^2}}, \tag{27a}$$

$$R_{3,c2}^{V} = \frac{k_4^2\sqrt{k_3^2 - k_2^2} - k_3^2\sqrt{k_4^2 - k_2^2}}{k_4^2\sqrt{k_3^2 - k_2^2} + k_3^2\sqrt{k_4^2 - k_2^2}}, \tag{27b}$$

$$R_{1,c4}^{H} = \frac{\sqrt{k_2^2 - k_4^2} - \sqrt{k_1^2 - k_4^2}}{\sqrt{k_2^2 - k_4^2} + \sqrt{k_1^2 - k_4^2}}, \tag{28a}$$

$$R_{2,c4}^{H} = \frac{\sqrt{k_3^2 - k_4^2} - \sqrt{k_2^2 - k_4^2}}{\sqrt{k_3^2 - k_4^2} + \sqrt{k_2^2 - k_4^2}}, \tag{28b}$$

$$R_{2,c4}^{V} = \frac{k_2^2\sqrt{k_1^2 - k_4^2} - k_1^2\sqrt{k_2^2 - k_4^2}}{k_2^2\sqrt{k_1^2 - k_4^2} + k_1^2\sqrt{k_2^2 - k_4^2}}, \tag{28c}$$

$$R_{2,c4}^{V} = \frac{k_3^2\sqrt{k_2^2 - k_4^2} - k_2^2\sqrt{k_3^2 - k_4^2}}{k_3^2\sqrt{k_2^2 - k_4^2} + k_2^2\sqrt{k_3^2 - k_4^2}}. \tag{28d}$$

A.2.1 Along the air-canopy interface

Substituted parameters are given by:

$$a_1 = e^{j2h_2H_1}[R_{2,c1}^{V} e^{j2h_3(z-H_2)} + 1], \tag{29a}$$

$$a_2 = e^{j2h_2H_1}[R_{2,c1}^{V} e^{j2h_3(z-H_2)} - 1], \tag{29b}$$

$$a_3 = e^{j2h_2H_1}[R_{2,c1}^{H} e^{j2h_3(z-H_2)} + 1], \tag{29c}$$

$$a_4 = e^{j2h_2H_1}[1 - R_{2,c1}^{V} e^{j2h_3(z'-H_2)}], \tag{29d}$$

$$a_5 = e^{j2h_2H_1}[R_{2,c1}^{V} e^{j2h_3(z'-H_2)} + 1], \tag{29e}$$

$$b_1 = k_1\rho + k_3[2(m+1)H_2 - z - z']\sqrt{1 - n_1^2}, \tag{30a}$$

$$b_2 = k_3\rho\sqrt{1 - n_1^2} - k_1[2(m+1)H_2 - z - z'], \tag{30b}$$

$$c_1 = e^{j2h_2H_1}[R_{3,c1}^{V} + R_{2,c1}^{V} e^{-j2h_3H_2}], \tag{31a}$$

$$c_2 = e^{j2h_2H_1}[R_{3,c1}^{H} + R_{2,c1}^{H} e^{-j2h_3H_2}], \tag{31b}$$

$$d_1 = R^V_{2,c1} R^V_{3,c1} - e^{j2h_2H_1}[R^V_{3,c1} + R^V_{2,c1} e^{-j2h_3H_2}], \tag{32a}$$
$$d_2 = e^{j2h_3(z-H_2)} + R^V_{2,c1} - e^{j2h_2H_1}[R^V_{2,c1} e^{j2h_3(z-H_2)} + 1], \tag{32b}$$
$$d_3 = e^{j2h_3(z-H_2)} - R^V_{2,c1} - e^{j2h_2H_1}[R^V_{2,c1} e^{j2h_3(z-H_2)} - 1], \tag{32c}$$
$$d_4 = e^{j2h_2H_1}[R^H_{3,c1} + R^H_{2,c1} e^{-j2h_3H_2}] + R^H_{2,c1} R^H_{3,c1}, \tag{32d}$$
$$d_5 = e^{j2h_2H_1}[R^H_{2,c1} e^{j2h_3(z-H_2)} + 1] + R^H_{2,c1} + e^{j2h_3(z-H_2)}, \tag{32e}$$
$$d_6 = R^V_{2,c1} - e^{j2h_3(z'-H_2)} - e^{j2h_2H_1}[1 - R^V_{2,c1} e^{j2h_3(z'-H_2)}], \tag{32f}$$
$$d_7 = e^{j2h_3(z'-H_2)} + R^V_{2,c1} - e^{j2h_2H_1}[R^V_{2,c1} e^{j2h_3(z'-H_2)} + 1], \tag{32g}$$

$$\Gamma_1 = 1 - R^V_{3,c1} e^{j2h_3z'}, \tag{33a}$$
$$\Gamma_2 = 1 + R^V_{3,c1} e^{j2h_3z'}, \tag{33b}$$
$$\Gamma_3 = 1 - R^H_{3,c1} e^{j2h_3z'}, \tag{33c}$$
$$\Gamma_4 = 1 - R^V_{3,c1} e^{j2h_3z}, \tag{33d}$$
$$\Gamma_5 = 1 + R^V_{3,c1} e^{j2h_3z}. \tag{33e}$$

A.2.2 Along the canopy-trunk interface

Substituted parameters are given by:

$$a_1 = 1 - e^{j2h_3(z-H_2)}, \tag{34a}$$
$$a_2 = 1 + e^{j2h_3(z-H_2)}, \tag{34b}$$
$$a_3 = 1 - e^{j2h_3(z'-H_2)}, \tag{34c}$$
$$a_4 = 1 + e^{j2h_3(z'-H_2)}, \tag{34d}$$

$$b_1 = k_2\rho + k_3[2(m+1)H_2 - z - z']\sqrt{1-n_2^2}, \tag{35a}$$
$$b_2 = k_3\rho\sqrt{1-n_2^2} - k_2[2(m+1)H_2 - z - z'], \tag{35b}$$

$$\Gamma_1 = 1 - R^V_{3,c2} e^{j2h_3z'}, \tag{36a}$$
$$\Gamma_2 = 1 + R^V_{3,c2} e^{j2h_3z'}, \tag{36b}$$
$$\Gamma_3 = 1 - R^H_{3,c2} e^{j2h_3z'}, \tag{36c}$$
$$\Gamma_4 = 1 - R^V_{3,c2} e^{j2h_3z}, \tag{36d}$$
$$\Gamma_5 = 1 + R^V_{3,c2} e^{j2h_3z}. \tag{36e}$$

A.2.3 Along the trunk-ground interface

Substituted parameters are given by:

$$a_1 = -e^{j2h_3z'}, \tag{37a}$$
$$a_2 = 1 - e^{j2h_3z'}, \tag{37b}$$
$$a_3 = R^V_{2,c4} + R^V_{1,c4}e^{j2h_2H_1} + R^V_{1,c4}R^V_{2,c4}e^{j2(h_2H_1-h_3H_2)}, \tag{37c}$$
$$a_4 = 1 + e^{j2h_3z'}, \tag{37d}$$
$$a_5 = R^H_{1,c4}R^H_{2,c4}e^{j2(h_2H_1-h_3H_2)} - R^H_{2,c4} - R^H_{1,c4}e^{j2h_2H_1}, \tag{37e}$$
$$a_6 = -e^{j2h_3z}, \tag{37f}$$
$$a_7 = 1 - e^{j2h_3z}, \tag{37g}$$
$$a_8 = e^{j2h_3z}, \tag{37h}$$
$$a_9 = 1 + e^{j2h_3z}, \tag{37i}$$

$$b_1 = k_4\rho + k_3[2(m+1)H_2 - z - z']\sqrt{1-n_4^2}, \tag{38a}$$
$$b_2 = k_3\rho\sqrt{1-n_4^2} - k_4[2(m+1)H_2 - z - z'], \tag{38b}$$

$$c_1 = R^V_{2,c4} + R^V_{1,c4}e^{j2h_2H_1}, \tag{39a}$$
$$c_2 = R^H_{2,c4} + R^H_{1,c4}e^{j2h_2H_1}, \tag{39b}$$

$$\Gamma_1 = (1 + R^V_{1,c4}R^V_{2,c4}e^{j2h_2H_1})e^{j2h_3(z-H_2)} + (R^V_{2,c4} + R^V_{1,c4}e^{j2h_2H_1}), \tag{40a}$$
$$\Gamma_2 = (1 + R^V_{1,c4}R^V_{2,c4}e^{j2h_2H_1})e^{j2h_3(z-H_2)} - (R^V_{2,c4} + R^V_{1,c4}e^{j2h_2H_1}), \tag{40b}$$
$$\Gamma_3 = (1 + R^H_{1,c4}R^H_{2,c4}e^{j2h_2H_1})e^{j2h_3(z-H_2)} + (R^H_{2,c4} + R^H_{1,c4}e^{j2h_2H_1}), \tag{40c}$$
$$\Gamma_4 = (R^V_{2,c4} + R^V_{1,c4}e^{j2h_2H_1}) - (1 + R^V_{1,c4}R^V_{2,c4}e^{j2h_2H_1})e^{j2h_3(z'-H_2)}, \tag{40d}$$
$$\Gamma_5 = (R^V_{2,c4} + R^V_{1,c4}e^{j2h_2H_1}) + (1 + R^V_{1,c4}R^V_{2,c4}e^{j2h_2H_1})e^{j2h_3(z'-H_2)}. \tag{40e}$$

REFERENCES

1. Tamir, T., "On radio-wave propagation in forest environments," *IEEE Trans. Antennas Propagat.,* Vol. AP-15, 806–817, November, 1967
2. Sachs, D. L., and P. J. Wyatt, "A conducting slab model for electromagnetic propagation within a jungle medium," *Radio Sci.,* Vol. 3, 125, 1968.
3. Dence, D., and T. Tamir, "Radio loss of lateral waves in forest environments," *Radio Sci.,* Vol. 4, 307, 1969.
4. Tamir, T., "Radio waves propagation along mixed paths in forest environments," *IEEE Trans. Antennas Propagat.,* Vol. AP-25, 471–477, July, 1977.
5. Cavalcante, G. P. S, D. A. Rogers, and A. J. Giardola, "Radio loss in forests using a model with four layered media," *IEEE Trans. Antennas Propagat.,* Vol. AP-31, 141–145, January, 1983.
6. Cavalcante, G. P. S., D. A. Rogers, and A. J. Giardola, "Radio loss in forests using a model with four layered media," *Radio Sci.,* Vol. 18, 691–695, 1983.
7. Seker, S. S., and A. Schneider, "Stochastic model for pulsed radio transmission through stratified forests," *IEE Proc. Microwave, Antennas & Propagat.,* Vol. 134, 361–368, 1987.
8. Seker, S. S., "Radio pulse transmission along mixed paths in a stratified forest," *IEE Proc. Microwave, Antennas & Propagat.,* Vol. 136, 13–18, 1989.
9. Tai, C. T., *Dyadi Green's Functions in Electromagnetic Theory,* IEEE Press, Piscataway, New Jersey, the 2nd edition, 1994.
10. Cavalcante, G. P. S., D. A. Rogers, and A. J. Giardola, "Analysis of the electromagnetic wave propagation in multilayered media using dyadic Green's function," *Radio Sci.,* Vol. 17, 503–508, 1982.
11. Li, L. W., J. A. Bennett, and P. L. Dyson, "Some methods for solving the coefficients of dyadic Green's function in isotropic stratified media," *Int. J. Electron.,* Vol. 70, No. 4, 803–814, 1991.
12. Li, L. W., P. S. Kooi, M. S. Leong, and T. S. Yeo, "On the eigenfunction expansion of dyadic Green's function in planarly stratified media," *J. Electromagn. Waves Applic.,* Vol. 8, No. 6, 663–678, June 1994.
13. Li, L. W, T. S. Yeo, P. S. Kooi, and M. S. Leong, "Radio wave propagation along mixed paths through a four-layered model of rain forest: An analytic approach," *IEEE Trans. Antennas Propagt.,* Vol. 46, No. 7, 1098–1111, July, 1998.

14. King, R. W. P., M. Owens, and T. T. Wu, *Lateral Electromagnetic Waves: Theory and Applications to Communications, Geophysical Exploration, and Remote Sensing,* Springer-Verlay, New York, 1992.
15. Brekhovskikh, L. M., *Waves in Layered Media,* Academic Press, New York, 1960.
16. Ishimaru, A., *Electromagnetic Wave Propagation, Radiation, and Scattering,* Prentice-Hall, New Jersey, 1991.
17. Arutaki, A., and J. Chiba, "Communication in three-layered conducting media with a vertical magnetic dipole," *IEEE Trans. Antennas Propagat.,* Vol. AP-28, 551–556, 1980.